JOURNAL OF DECISION MAKING AND HEALTHCARE
Volume 3 (2026), No. 1, 21–31
https://doi.org/10.69829/jdmh-026-0301-ta02
Tulipa Opera Scholarum

# THE ROLE OF EVOLVING SHORT AND LONG-TERM WEATHER PATTERNS ON IRRIGATIVE WATER DEMAND IN THE U. S. NORTHEAST AND MID-ATLANTIC USING AUTOREGRESSIVE INTEGRATED MOVING AVERAGE TIME SERIES MODELING AND RANDOMIZED HISTORICAL DATA

ROBERT KENNEDY SMITH[1] AND DER-CHEN CHANG[1,*]

[1] *Department of Mathematics and Statistics, Georgetown University, Washington, DC, USA*

Abstract. Historical data records show that annual and seasonal precipitation have increased in the U.S. Northeast and Mid-Atlantic over the past several decades, with higher rates evident more recently. Climate models project continuing growth in precipitation through the rest of the century. The same models also predict more frequent, intense precipitation episodes, during which soils may not be able to fully absorb water hitting the ground, and higher evapotranspiration rates, leading to increased dryness despite higher rainfall totals. This analysis uses autoregressive integrated moving average modeling to examine the impacts of short and long-term weather patterns on soil moisture levels in the Region, some of which are not explicitly accounted for in decadal climate modeling. Comparisons of calculated soil moisture utilizing historical and randomized data show that such patterns are causing increased dryness that will exacerbate soil water deficits beyond what is already projected from increased evapotranspiration and runoff.

**Keywords.** Precipitation, Evapotranspiration, Soil moisture, ARIMA, Drought.



## 1. Introduction and Background

The Northeast and Mid-Atlantic United States have experienced increased average annual precipitation over recent decades [14], with wetter summers and winters [12]. The region covered by this analysis, located between the Appalachian Highlands to the West and Atlantic Ocean to the East, houses several large metropolitan areas, forests, and farms (Figure 1) [15]. It receives relatively uniform amounts of annual precipitation, but highly variable snowfall: the warmest and least snowy location included, Norfolk International Airport, receives 157 mm (6.2 inches) in an average winter, while in the snowiest, Albany International Airport, 1504 mm (59.20 inches) can be expected. There is a high degree of consensus and confidence among climate models that greater amounts of precipitation will continue to fall in an average year through the late 21st century, regardless of the level of future temperature increase [12]. Under an intermediate warming scenario, even the driest 20 percent of model projections anticipate a modest increase in annual rainfall through midcentury, relative to current amounts [13]. Exhaustive explanations for the projected increases are not covered in this analysis, but warming sea surface temperatures have strengthened the large-scale extratropical cyclones that affect the region during the cool season (locally called Nor'easters for their moist winds off the Atlantic Ocean) [3]. Tropical cyclones and their remnants wet the Northeast and Mid-Atlantic in the summer and fall, and research shows these systems are strengthening relative to the mid-20th century average, hitting inland locations more frequently rather than curving out into the Atlantic [18], and moving more slowly after impacting the East Coast [6]. Such factors differentiate this area from the rest of the contiguous U.S. [4].

*Corresponding author.
E-mail address: rks21383@gmail.com (R. K. Smith) and chang@georgetown.edu (D.-C. Chang)
Accepted: February 08, 2026.

As anthropogenic warming has enhanced precipitation amounts, it has also increased the number of extreme episodes during which rainfall exceeds soil absorption rates and event totals surpass soil water holding capacity [9, 16]. Moreover, water leaving the soil from higher evapotranspiration (ET) rates due to warmer temperatures is expected to approximate or exceed precipitation increases before midcentury [13], leaving vegetation vulnerable to desiccation [2]. The model consensus projects that enhanced atmospheric evaporative demand (AED) will result in more severe water deficits by 2050, leading to lower soil moisture levels during the lengthening growing season [7, 13, 11].

During summertime in the southern portion of the region, potential, or reference, evapotranspiration can approach values of 10 mm per day (9 mm per day in the North). At such high rates, even saturated soils can exhaust their readily available water supply within a few days, quickly causing stress to vegetation. Such flash droughts have and are projected to become more frequent under warmer conditions [10], exacerbated by more sporadic rainfall. Seasonal forecasts miss these events, as a month with above average rainfall can still experience devastating drought.

Using a daily recursive algorithm with imputed historical climate data, this analysis calculates the level of moisture in soil and quantifies the amount of hypothetical irrigation (supplemental) water needed to keep a standard grassy surface fully watered, so that the actual evapotranspiration rate (ET) matches the reference rate ($ET_0$). Monthly precipitation data is then randomized within the boundaries of each respective month, and the resulting supplemental water trends are compared to those calculated from historical data. The same process is repeated for three-year blocks of the same month. The results demonstrate the amount of drying attributed to evolving short and long-term weather patterns that cannot easily be quantified using global forecasting models. Recently, convolutional neural networks and other AI models have successfully downscaled precipitation timeframes to show intra-monthly impacts of warming [8, 5]. This analysis reinforces the importance of using granular timescales to accurately measure soil moisture deficits.

## 2. Algorithm Methodology

To calculate soil moisture in the recursive algorithm, four climate parameters were used: wind speed (m $s^{-1}$), solar radiation [MJ $m^{-2}$ $day^{-1}$], air temperature (°C), and dewpoint temperature (°C). Data originated from the National Centers for Environmental Information (NCEI) and the North American Regional Reanalysis (NARR), an extension of the NCEP Global Reanalysis. Precipitation amounts were also provided by NCEI. The FAO-56 Penman–Monteith equation for reference evapotranspiration ($ET_0$) [19] was then deployed to calculate the amount of water that leaves soils covered by a uniform reference surface. It is given by the following:

$$ET_0 = \frac{0.408\Delta(R_n - G) + \gamma\frac{900}{T+273}u_2(e_s - e_a)}{\Delta + \gamma(1 + 0.34u_2)} \tag{2.1}$$

where $\Delta$ is the slope of the saturation vapor pressure curve, $R_n$ is the net radiation at the crop surface, $G$ is the soil heat flux density, $\gamma$ is the psychrometric constant, $T$ is the mean daily air temperature, $u_2$ is the wind speed, $e_s$ is the saturation vapor pressure, and $e_a$ is the actual vapor pressure.

In the Northeast and Mid-Atlantic, there were 20 observation sites that exceeded 99.5 percent coverage for the prerequisite climate data (Figure 1). At each location, a weighted average of the moisture holding capacity in the top meter of soil was found with the USDA National Resources Conservation Service's online soil survey. Forty percent of this total was assumed to be readily available for surface

https://data.noaa.gov/dataset/global-surface-summary-of-the-day-gsod; https://www.ncdc.noaa.gov/data-access/land-based-station-data/land-based-datasets/global-historical-climatology-network-ghcn

http://climateengine.org/

The reference surface is well-watered fescue grass mowed at a height of 0.12 meters. It is assumed to be dormant when the daily average temperature remains below 4.4°C.

vegetation [17]. Days during which precipitation fell replenished the soil's water supply until its field capacity was exceeded. Additional water was assumed to flow off the surface and be unavailable by the next day. To estimate the surface grass' supplemental moisture requirements, 12.7 mm (1/2") of water was introduced into the algorithm at the time of readily available supply depletion. This quantity was summed over each month from January 1979 through December 2024.

The impact of short-term weather patterns on water scarcity was quantified by repeating the same procedure, but with each month's daily precipitation amounts randomized over that month. Even though totals and the number of wet days remained equal for each of the 552 months, the days on which precipitation fell differed. A comparison of supplemental water trend magnitudes between the average of 12 randomized set procedures and the observed data record provides insight into how intramonthly patterns are changing water demand. Precipitation occurrences in three-year blocks were also randomized to measure the impact of long-term patterns. That is, the precipitation falling in each block of three consecutive Januarys, Februarys, etc. was randomized, with the average trends from 12 randomizations also compared to the historical ones. Whereas the first randomization accounts for short-term occurrences like flash drought episodes, the later process determines the impacts of seasonal patterns such as the El Niño–Southern Oscillation (ENSO).

## 3. Model Selection

One effective way to measure the magnitude of trends in the time series data comprising the monthly water demand to preserve the grass covering in a well-watered state would be to run the autocorrelation function of the residuals from a classic linear regression on seasonally adjusted records and determine the appropriate lags to add to the model until none of the residuals from the subsequent regression showed statistically significant correlation. However, the comparisons used in this analysis require a more precise and standardized procedure since there is considerable volatility and subjectivity in the visual inspection of residuals and determining which lagged parameters to include. Data comprised with randomized precipitation will still exhibit correlations, but they are weaker since the procedure partially neutralizes established weather patterns. In this way, the historical baseline is more strongly correlated than randomized modifications, making direct comparisons of trends from linear regressions difficult. Therefore, autoregressive integrated moving average (ARIMA) models were deployed using the Akaike Information Criterion (AIC) for model selection in R. An ARIMA model, which results in stationary data, is given by the following:

$$ARIMA(p, d, q) \tag{3.1}$$

where $p$ is the autoregressive (AR) order, $d$ is the order of integration by differencing (I), and $q$ is the moving average (MA) order. The function `auto.arima` in R automatically calculates each optimal order.

While ARIMA models are amiable to the comparisons used in this analysis, they achieve stationarity through detrending processes. A drift, however, remains, and drifts between observed and randomized data were calculated and evaluated. The difference in magnitude between a linear trend $\beta_1$, in the classic time series regression

$$Z_t = \beta_0 + \beta_1 t + w_t \tag{3.2}$$

If readily available water was depleted on a rainy day, the amount of precipitation was subtracted from 12.7 mm. If 12.7 mm was exceeded, no water was introduced on that day.

The observed depth of rainfall on each calendar date was not modified; only the dates were randomized

https://www.r-project.org/

and the ARIMA drift term $\delta$ is not explicit, but is explored in the Results and Discussion Section with an example. However, if $Z_t$ is modified so that

$$Z_t^* = Z_t + t \tag{3.3}$$

(that is, an additional unit is added to each $Z_t$ for each subsequent timestep), both the regression coefficient and drift estimates increase by one unit.

## 4. Results and Discussion

Historical precipitation between 1979 and 2024 has increased at all 20 observation locations, in line with current findings. The mean increase was 40.9 mm per decade (range: 4.6–114 mm per decade) using classic linear regressions with autocorrelation lags, and 2.9 mm per decade (range: 0.7–6.9 mm per decade) from the drift component of ARIMA modeling. Assumed historical water usage to preserve well-watered vegetation as calculated by the soil moisture algorithm and classic linear regression declined at 15 of 20 stations, with a mean decrease of 9.5 mm per decade across all sites (range: 28.5 mm decrease – 17.0 mm increase). With drift from ARIMA modeling, water demand also declined at 15 stations, with an average decrease of 1.0 mm per decade (range: 3.9 mm decrease – 1.7 mm increase). Thus, the rainfall trend magnitude was 14 times greater with a classic regression relative to the ARIMA drift while watering demand was 9.5 times greater. Some context of these discrepancies is provided: when NOAA released their 1981–2010 annual precipitation normals, the average increase across the 20 reporting locations was 0.5 mm compared with the 1971–2000 period. However, the mean increase between the 1981–2010 normals and the 1991–2020 update was 38.7 mm. While the latest release closely tracks with the increase estimated by linear regression, the earlier wetting was negligible. Since ARIMA modeling measures drift after achieving stationarity, some of the trend is inevitably lost; therefore, the subsequent results are an underestimation of the observed magnitude. The reader is encouraged to focus on the overall signals from the ARIMA drift comparisons rather than on specific magnitudes, as all subsequent results summarize differences in drift rather than linear regression trends. However, "trend" will now be used synonymously with "drift" when reporting the results.

The average of 12 sets of randomized monthly precipitation shows a larger decrease or smaller increase with time for supplemental water demand than the historical baseline at 17 of 20 stations, and of the three stations where the randomized data results in accelerated drying, only one has a net increase of more than 0.1 mm per decade. Differences between the annual rate of change in demand based on hypothetical historical and randomized watering data are shown in Figure 2 for each station, organized from left to right by increasing latitude. Due to increasing precipitation, most stations have a negative demand for supplemental water with time and lie below zero on the y-axis. The vertical distance between the two points at each station represents the difference in the slope (mm per year) between the historical and simulated data trends. Figure 3 shows the spread of the 12 simulations for the corresponding sites, with each box representing the interquartile range (middle six values). Each station's mean and median is represented by an "X" and horizontal line, respectively. Therefore, each "X" aligns with Figure 2's blue dot at all 20 locations.

Figure 4 extends the difference in trend magnitudes over the 46-year analysis period. Each of the 20 colored circles represents the expected difference in irrigative water demand between the observed record and the 12 randomized intramonthly simulations at the conclusion of the analysis period in an average or typical year. No difference is represented by grayscale shading in the circle. If the historical pattern resulted in increased supplemental water relative to the simulated trends, the circle's fill becomes a more vibrant shade of violet as the magnitude of the difference of the drift increases. In contrast, if drifts from simulated data resulted in accelerated drying, the circle's hue moves in the opposite direction and becomes greener. The prevalence of violet shading in the Figure demonstrates

https://ggweather.com/normals

how evolving short-term patterns are increasing aridity compared to random simulations utilizing the same monthly precipitation totals and number of wet days. As noted, the historical trend in reduced irrigation water demand was found to be 1.0 mm per decade, so the modeled demand under average conditions in 2024 would be a 4.6 mm decline relative to initial average conditions. In contrast, the decadal randomized trend is 1.2 mm, so average conditions in 2024 would require 5.4 mm less water than 1979 average demand. In plain language: the randomized data results in a 13% reduction in water usage when compared to the historical baseline; or, evolving short-term precipitation patterns have eliminated 13% of the wetting that would otherwise have been expected by accounting for the difference between monthly precipitation and $ET_0$ trends.

When precipitation occurrences are randomized in three-year blocks of the same month, there is higher variability in the difference of trend magnitudes with respect to the historical data (Figures 5 and 6). As with the intramonthly randomizations, 17 of 20 stations show a larger decrease or smaller increase with time for supplemental water demand under the block simulations than with historical data; there is just higher volatility. Figure 7 shows the same comparison as in Figure 4, with the 3-year monthly block randomizations instead contrasted with the observed baseline. Although the block trend is slightly larger than the intramonthly one, it also rounds to 1.2 mm, and average 2024 conditions would require 5.5 mm less water than in 1979. This randomization results in a 15% reduction in demand relative to the historical records, meaning that the combined impact of short and long-term weather patterns have nullified 15% of the wetting that otherwise would have occurred. There is therefore little additional impact on drying from long-term patterns, although if outlier Norfolk International Airport is excluded from the historical and simulated averages, the 15% wetting offset would grow to 21%.

A final note: as shown in Figures 3 and 6, randomized simulations result in variable supplemental water trends/drifts. When comparing the trends of historical data in Figure 2 to the height of the whiskers in Figure 3 for each station, it is common for trends resulting from different simulations to be less than or greater than the reference historical value, based on random probability. By performing 12 randomization simulations, the true value of the mean from an infinite number of processes was approximated but never obtained, as manual entry into R required a manageable process. Since many of the differences between the historical and simulated drifts were very small, it is possible that some of them could flip if additional simulations were conducted, but changes to the overall percentage differences would be so slight, they would remain hidden as rounding errors.

## 5. Conclusion

While the Northeast and Mid-Atlantic United States have seen increased annual, seasonal, and monthly precipitation totals with time, an analysis of soil moisture shows that the amount of irrigation needed to maintain a well-watered surface covering has decreased less than the amount of water hitting the ground. This is primarily due to increased $ET_0$ rates from warmer temperatures, but precipitation intensity, amounts, and timing have also contributed to longer, more frequent, and more intense dry periods. While long-term global patterns are well represented in climate forecasts, effective spatial and temporal downscaling offers challenges to current computing methods [1]. This analysis shows that evolving frequency and amounts of intramonthly precipitation events have caused a 13-percent increase in vegetative water demand (or, in more precise language, nullified 13 percent of the total decrease in assumed irrigative water demand resulting from increasing rainfall amounts). Climate projections should include discussions on evolving intramonthly patterns, as no monthly rain and snow totals were changed in the short-term portion of this analysis, yet almost every station experienced reduced drought mitigation benefits relative to randomized event placement scenarios. Long-term patterns, better captured in existing models, have less of an influence in the Northeast and Mid-Atlantic. No correlations of findings with observation site latitude were noted. Accounting for and communicating the growing impact of short-term patterns on agricultural drought and related water demand


FIGURE 1. Northeast and Mid-Atlantic United States, with data observation locations denoted by a black diamond

will become essential for effective infrastructure and land-use planning, even in a region with relative water abundance like the Northeast and Mid-Atlantic U.S.

## STATEMENTS AND DECLARATIONS

The authors declare that they have no conflict of interest, and the manuscript has no associated data.

## ACKNOWLEDGMENTS

Der-Chen Chang's research is partially supported by a National Science Foundation grant (DMS-1408839) and the McDevitt Endowment Fund at Georgetown University.

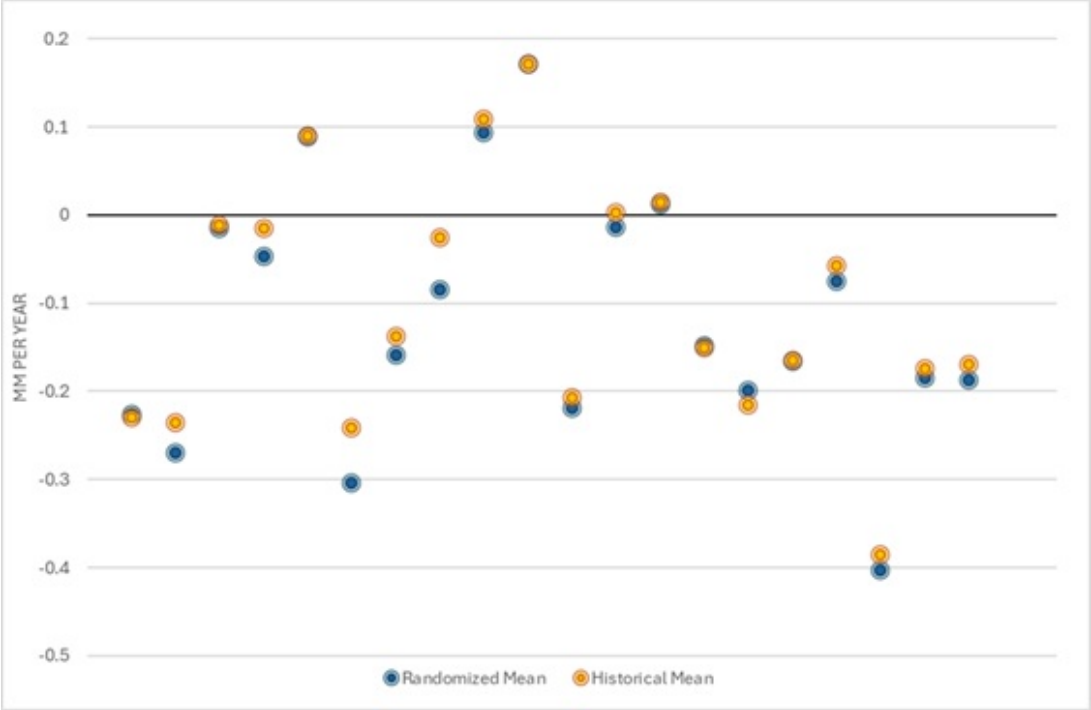


FIGURE 2. Difference in the annual rate of change in assumed supplemental water demand from the soil moisture algorithm using historical data and the mean of 12 randomized intramonthly precipitation patterns

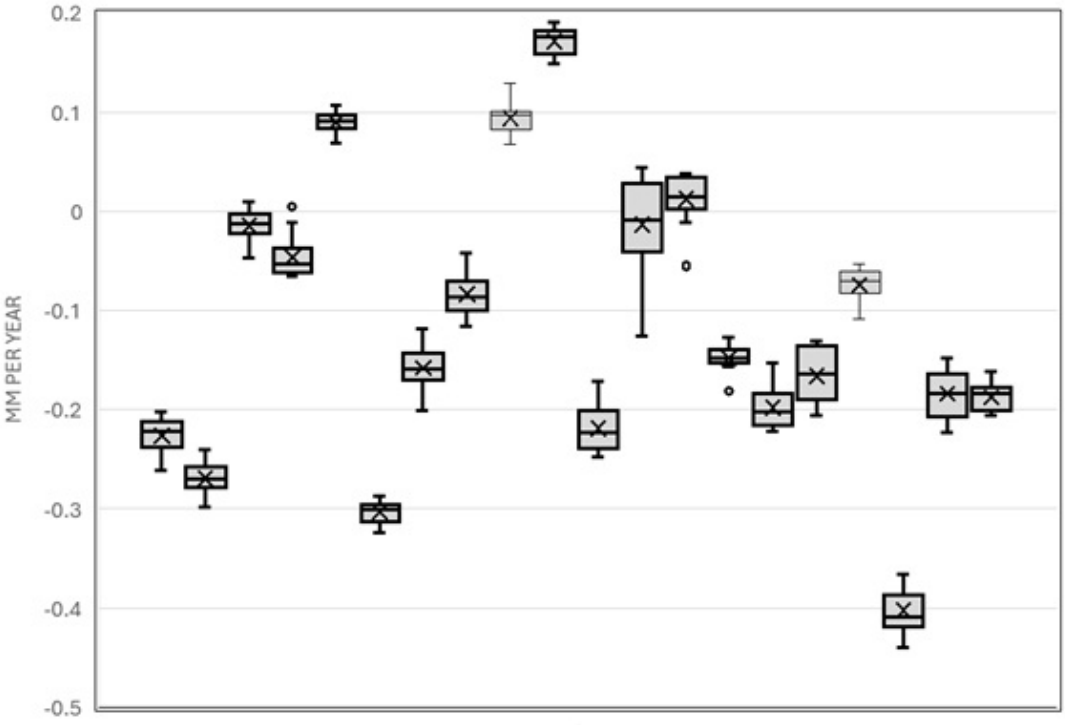


FIGURE 3. The range of supplemental water trend magnitudes for the 12 intramonthly randomized precipitation simulations

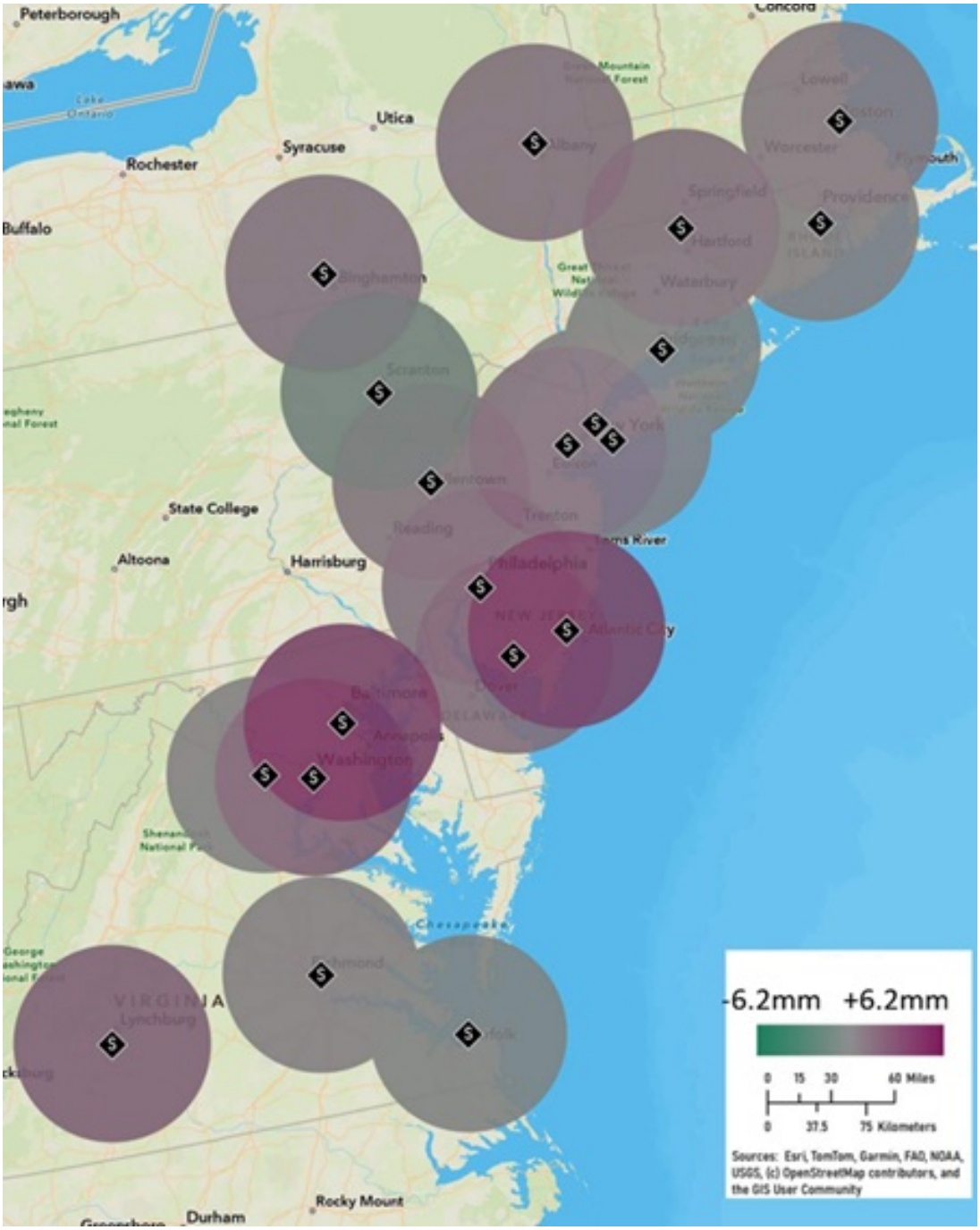


FIGURE 4. Modeled change in assumed supplemental water demand for an average year at the end of the analysis period relative to modeled demand from the mean of intramonthly randomized precipitation simulations in the same year

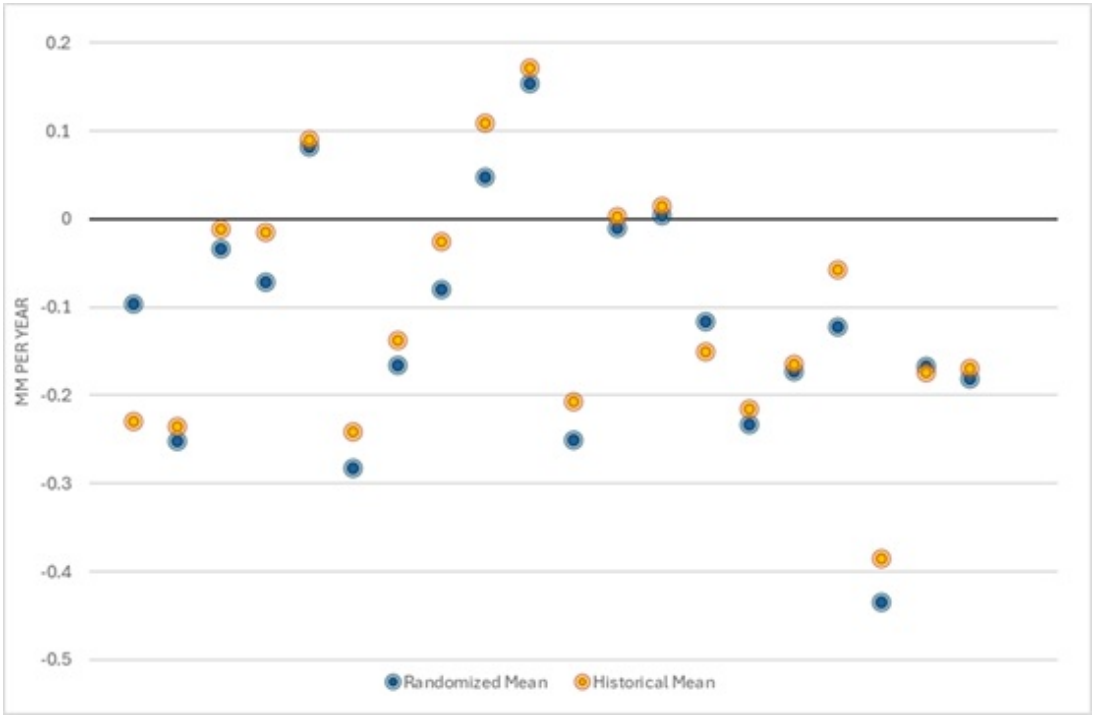


FIGURE 5. Difference in the annual rate of change in assumed supplemental water demand from the soil moisture algorithm using historical data and the mean of 12 randomized 3-year precipitation blocks

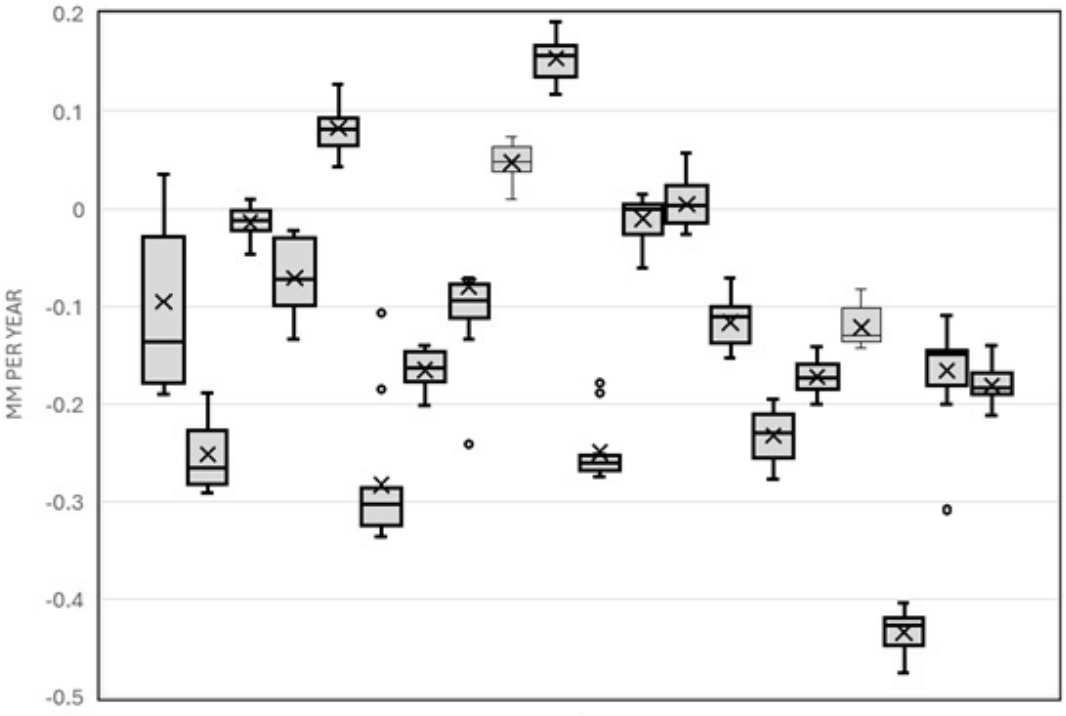


FIGURE 6. The range of supplemental water trend magnitudes for the 12 randomized 3-year precipitation blocks simulations

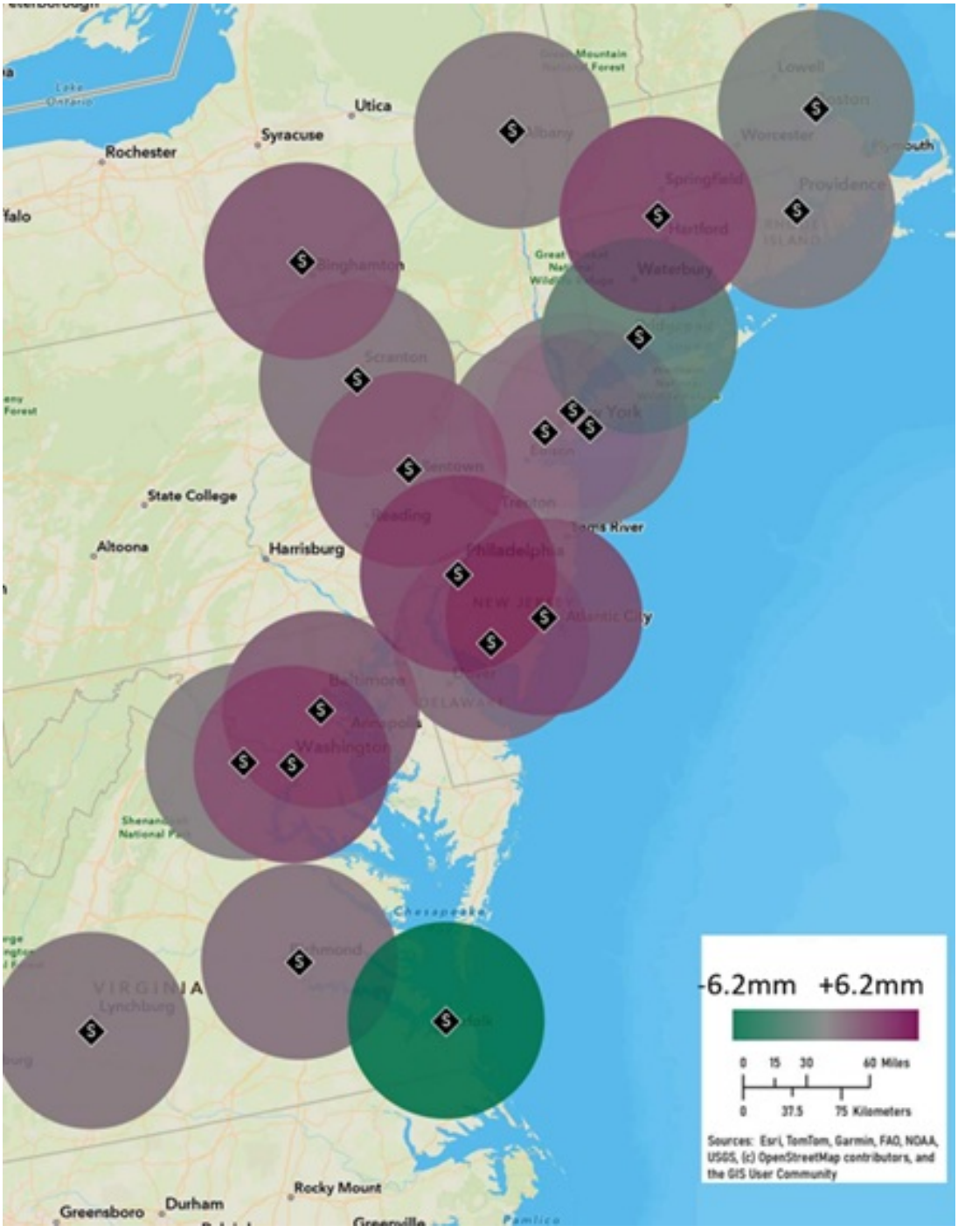


FIGURE 7. Modeled change in assumed supplemental water demand for an average year at the end of the analysis period relative to modeled demand from the mean of randomized three-year monthly block precipitation simulations in the same year

## References


[1] O. Alizadeh. Advances and challenges in climate modeling. *Climatic Change*, 170:Article ID 18, 2022. https://doi.org/10.1007/s10584-021-03298-4

[2] M. J. Alessi, D. A. Herrera, C. P. Evans, A. T. DeGaetano, and T. R. Ault. Soil moisture conditions determine land–atmosphere coupling and drought risk in the Northeastern United States. *Journal of Geophysical Research: Atmospheres*, 127(6):Article ID e2021JD034740, 2022. https://doi.org/10.1029/2021JD034740

[3] K. Chen, X. Li, M. M. Weaver, S. A. Christiansen, A. L. Horton, and M. E. Mann. The intensification of the strongest nor'easters. *Proceedings of the National Academy of Sciences*, 122(29):Article ID e2510029122, 2025. https://doi.org/10.1073/pnas.2510029122

[4] D. R. Easterling, K. E. Kunkel, J. R. Arnold, T. Knutson, A. N. LeGrande, L. R. Leung, R. S. Vose, D. E. Wal- iser, and M. F. Wehner. Precipitation change in the United States. In, D. J. Wuebbles, D. W. Fahey, K. A. Hibbard, D. J. Dokken, B. C. Stewart, and T. K. Maycock, editors, *Climate Science Special Report: Fourth National Climate Assessment*, Volume I, pages 207-230. U. S. Global Change Research Program, Washington, USA. https://doi.org/10.7930/J0H993CC

[5] V. Eyring, W. D. Collins, P. Gentine, E. A. Barnes, M. Barreiro, T. Beucler, M. Bocquet, C. S. Bretherton, H. M. Christensen, K. Dagon, D. J. Gagne, D. Hall, D. Hammerling, S. Hoyer, F. Iglesias-Suarez, I. Lopez-Gomez, M. C. McGraw, G. A. Meehl, M. J. Molina, C. Monteleoni, J. Mueller, M. S. Pritchard, D. Rolnick, J. Runge, P. Stier, O. Watt-Meyer, K. Weigel, R. Yu, and L. Zanna. Pushing the frontiers in climate modelling and analysis with machine learning. *Nature Climate Change*, 14:916–928, 2024. https://doi.org/10.1038/s41558-024-02095-y

[6] A. Garner, R. Kopp, and B. Horton. Evolving tropical cyclone tracks in the North Atlantic in a warming climate. *Earth's Future*, 9(12):Article ID e2021EF002326, 2021. https://doi.org/10.1029/2021EF002326

[7] S. H. Gebrechorkos, J. Sheffield, S. M. Vicente-Serrano, C. Funk, D. G. Miralles, J. Peng, E. Dyer, J. Talib, H. E. Beck, M. B. Singer, and S. J. Dadson. Warming accelerates global drought severity. *Nature*, 642:628–635, 2025. https://doi.org/10.1038/s41586-025-09047-2

[8] Y. G. Ham, J. H. Kim, S. K. Min, D. Kim, T. Li, A. Timmermann, and M. F. Stuecker. Anthropogenic fingerprints in daily precipitation revealed by deep learning. *Nature*, 622:301–307, 2023. https://doi.org/10.1038/s41586-023-06474-x

[9] R. D. Harp and D. E. Horton. Observed changes in daily precipitation intensity in the United States. *Geophysical Research Letters*, 49(19):Article ID e2022GL099955, 2022. https://doi.org/10.1029/2022GL099955

[10] K. Lesinger and D. Tian. Trends, variability, and drivers of flash droughts in the contiguous United States. *Water Resources Research*, 58:Article ID e2022WR032186, 2022. https://doi.org/10.1029/2022WR032186

[11] Y. Liu, Z. Li, Y. Chen, L. Jin, F. Li, X. Wang, Y. Long, C. Liu, and P. Mindje. Global greening drives significant soil moisture loss. *Communications Earth & Environment*, 6:Article ID 600, 2025. https://doi.org/10.1038/s43247-025-02470-3

[12] K. Marvel, W. Su, R. Delgado, S. Aarons, A. Chatterjee, M. E. Garcia, Z. Hausfather, K. Hayhoe, D. A. Hence, E. B. Jewett, A. Robel, D. Singh, A. Tripati, and R. S. Vose. Climate trends. In A. R. Crimmins, C. W. Avery, D. R. Easterling, K. E. Kunkel, B. C. Stewart, and T. K. Maycock, editors, *Fifth National Climate Assessment*, Chapter 2. U. S. Global Change Research Program, Washington, USA, 2023. https://doi.org/10.7930/NCA5.2023.CH2.

[13] E. A. Payton, A. O. Pinson, T. Asefa, L. E. Condon, L.-A. L. Dupigny-Giroux, B. L. Harding, J. Kiang, D. H. Lee, S. A. McAfee, J. M. Pflug, I. Rangwala, H. J. Tanana, and D. B. Wright. Water. In A. R. Crimmins, C. W. Avery, D. R. Easterling, K. E. Kunkel, B. C. Stewart, and T. K. Maycock, editors, *Fifth National Climate Assessment*, Chapter 4. U. S. Global Change Research Program, Washington, USA, 2023. https://doi.org/10.7930/NCA5.2023.CH4

[14] C. J. Picard, J. M. Winter, C. Cockburn, J. Hanrahan, N. G. Teale, P. J. Clemins, and B. Beckage. Twenty-first century increases in total and extreme precipitation across the Northeastern USA. *Climatic Change*, 176:Article ID 72, 2023. https://doi.org/10.1007/s10584-023-03545-w

[15] S. K. Sweet, D. W. Wolfe, A. DeGaetano, and R. Benner. Anatomy of the 2016 drought in the Northeastern United States. *Agricultural and Forest Meteorology*, 247:571-581, 2017. https://doi.org/10.1016/j.agrformet.2017.08.024

[16] J. C. Whitehead, E. L. Mecray, E. D. Lane, L. Kerr, M. L. Finucane, D. R. Reidmiller, M. C. Bove, F. A. Montalto, S. O'Rourke, D. A. Zarrilli, P. Chigbu, C. C. Thornbrugh, E. N. Curchitser, J. G. Hunter, and K. Law.Ch. 21, Northeast. In A. R. Crimmins, C. W. Avery, D. R. Easterling, K. E. Kunkel, B. C. Stewart, and T. K. Maycock, Editors, *Fifth National Climate Assessment*. U.S. Global Change Research Program, Chapter 21, Washington, USA, 2023. https://doi.org/10.7930/NCA5.2023.CH21

[17] J. Wright. Nongrowing season evapotranspiration from irrigated fields. In *Management of Irrigation and Drainage Systems: Integrated Perspectives*, pages 1005–1014. American Society of Civil Engineers, Reston, United States.

[18] G. Zhang, H. Murakami, T. R. Knutson, R. Mizuta, and K. Yoshida. Tropical cyclone motion in a changing climate. *Science Advances*, 6(17):Article ID eaaz7610, 2020. https://doi.org/10.1126/sciadv.aaz7610

[19] L. Zotarelli, M. D. Dukes, C. C. Romero, K. W. Migliaccio, and K. T. Morgan. Step-by-step calculation of the Penman–Monteith evapotranspiration (FAO-56 method). University of Florida IFAS Extension, AE459, 2010.